American Journal of Mechanical Engineering, 2016, Vol. 4, No. 4, 131-141
Available online at http://pubs.sciepub.com/ajme/4/4/2

DOI:10.12691/ajme-4-4-2

Experimental Investigations of Surface Modification of AISI 1045 Die Steel by Electro Discharge Machining Process

Harjot Singh*, S.S. Banwait

Department of Mechanical Engineering, National Institute of Teachers Training and Research, Chandigarh, India
*Corresponding author: singhharjotbansal@gmail.com

Abstract In the present work Electric discharge machining process has been used for surface modification of AISI 1045 Die steel with copper chromium (Cu Cr) electrodes (made through powder metallurgy technique) by varying different machining parameters such as peak current, pulse on-time, pulse off-time and compaction pressure. Parametric optimization of Surface Deposition Rate, Surface Roughness and Micro Hardness was carried out by using Central Composite Design technique. Material characterization was also performed using X-Ray Diffraction and Scanning Electron Microscope to study the structure of the modified surface layer. It has been found that hardness increases by two times as compared to the base material. By the use of copper-chromium composite electrode, chromium particles gets collected on the surface which modified the work piece surface by increasing its corrosion and wear resistance The input process parameter pulse off-time has greater effect on surface deposition rate followed by peak current, pulse on-time and compaction pressure respectively.

Keywords: *electro discharge machining, surface modification, surface roughness and micro hardness*

Cite This Article: Harjot Singh, and S.S. Banwait, "Experimental Investigations of Surface Modification of AISI 1045 Die Steel by Electro Discharge Machining Process." *American Journal of Mechanical Engineering*, vol. 4, no. 4 (2016): 131-141. doi: 10.12691/ajme-4-4-2.

1. Introduction

Electro Discharge Machining is an electro-thermal non-traditional machining process where electrical energy is used to generate an electrical spark and material removal mainly occurs due to the thermal energy of the spark. EDM is mainly used to machine difficult-to-machine materials and high strength temperature resistant alloys. EDM can be used to machine difficult geometries in small batches or even on the job-shop basis. Work material to be machined by EDM has to be electrically conductive.

Surface modification using EDM is a technique in which tool electrode is used as an anode and workpiece is selected as cathode in EDM (polarity opposite to the electrical discharge machining) process and in the presence of dielectric fluid, material is decomposed from the tool electrode and deposited over the workpiece surface.

2. Literature Review

Many researchers have tried surface modification of different materials but very limited attempt has been made on surface modification of AISI 1045 Die Steel material. Some of the prominent work in this area is discussed below.

Patowari et al. [1] has enhanced the surface properties of engineering components of C-40 steel using W–Cu powder metallurgy electrodes by EDM process. The variations of mass transfer rate (MTR), deposited layer thickness (LT) and average surface roughness (Ra) with various parameter combinations were presented in graphical form and their effects were discussed. SEM, EDX and XRD analyses were performed for further characterization of the deposited layer. A quantitative analysis of the layer was carried out by EDX and found that the inner part of the layer was richer in tungsten than the superficial surface. Hayakawa et al. [2] described a metal deposition process using micro electrical discharge machining (micro EDM) to fabricate micro structures. Steel is used for the tool electrode and the EDM process is carried out in the air. It is observed from the discharging surface that the local gap distance of a discharge location becomes larger than that at other locations on the discharging surface and therefore the discharge points are not concentrated at a single point but distributed over the discharging surface. Patowari et al. [3] studied an experimental research on surface modification during electrical discharge machining (EDM) by depositing a hard layer over the work surface of C-40 grade plain carbon steel using specially prepared powder metallurgy compact tools. The investigated process parameters were composition, compaction pressure, sintering temperature, pulse on-time, peak–current setting and duty factor. Different studies like X-ray diffraction, optical microscopy, scanning electron microscopy and energy dispersive X-ray spectroscopy. Singh et al. [4] investigated the effect of addition of graphite powder in dielectric on the surface

properties of superalloy, Super Co 605 in electrical discharge machining process. The results showed that an optimization between micro hardness and surface finish could be achieved by this method of machining. Scanning electron microscope (SEM) images of the surface revealed a smoother surface and spectroscopy analysis indicated substantial increase in carbon percentage. Gill et al. [5] investigated the phenomenon of surface alloying by electrical discharge machining process using tool electrodes manufactured by powder metallurgy process. Different techniques like scanning electron microscopy (SEM), energy-dispersive spectroscopy (EDS) and X-ray diffraction (XRD) were used to ascertain the characteristics of the machined surface. The XRD shows the formation of cementite (Fe_3C) and tungsten carbide (W_3C) on the machined surface which was responsible for the substantial increase in micro hardness. SEM shows a crack free surface which indicated that surface alloying was carried out without any adverse impact on surface quality. Sidhu et al. [6] modified surface layer by using reverse polarity semi sintered powder metallurgy tool electrode which was an uncommon aspect of electrical discharge machining process. In this work, attempts were made to model the surface modification phenomenon by electrical discharge machining process with response surface methodology technique. Two output response parameters, surface deposition rate and surface roughness were correlated with four input variables peak discharge current, pulse-on time, pulse-off time, powder compaction pressure and good results were obtained. Abhishek Abrol et al. [7] found the effect of chromium powder mixed dielectric fluid on machining characteristics of AISI D2 die steel. Peak current, pulse on-time, pulse off-time, concentration of powder were the process parameters. The research outcome identified the important process parameters that maximize MRR, minimize TWR and SR.

Most of the researchers have analysed the surface modification by powder mixed electrode or powder suspended in dielectric fluid method. The researchers have carried out work on EDM developments, monitoring and control but very scant work has been reported on surface deposition on AISI 1045 die steel. The effect of machining parameters such as peak current, pulse on-time, pulse-off time, sintering temperature and pressure on AISI 1045 die steel has not been fully explored using EDM with powder metallurgy sintered electrode of copper-chromium.

3. Experimental Methodology

The effect of input parameters on the response parameters were estimated by developing appropriate methodology for finding an optimum solution for the desired surface modification of AISI 1045 die steel.

3.1. Electrode Material

Chromium is a lustrous, brittle and hard metal. It does not tarnish in air, when heated it burns and forms the green chromic oxide. Chromium is unstable in oxygen, it immediately produces a thin oxide layer that is impermeable to oxygen and protects the metal below.

Copper has been frequently used as electrode on a wire EDM. Significant disadvantages associated with Copper electrodes are:

- They generally burn only half as fast as graphite electrodes.
- Copper is a soft and gummy material to machine or grind.
- Copper is an extraordinarily difficult material to de-burr.

3.2. Powder Mixed Chromium-copper

The electrodes were prepared by powder metallurgy method. Copper and chromium in powdered form in desired proportion were manually mixed in the V-blender and the resultant powder was compressed with the help of hydraulic press. Sample of fabricated electrodes are shown in Figure 1.

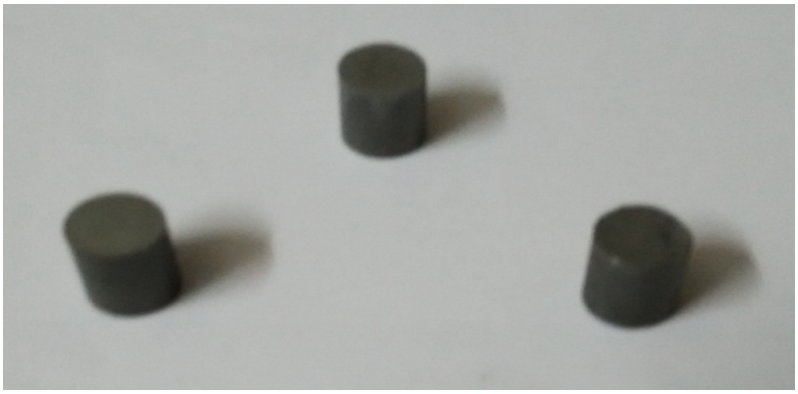

Figure 1. Fabricated Cu-Cr Electrode

Three sample electrodes of 10 mm height and 10 mm diameter of cylindrical shape were prepared. The faces of these electrodes were parallel and had shiny surface. The electrodes were prepared by sintering process at a particular sintering temperature and sintering pressure. The properties of copper and chromium are given in the Table 1.

Table 1. Properties of Copper and Chromium

Properties	Chromium	Copper
Density	7.19 g/cm^3 at 20°C	8.9 g/cm^3 at 20°C
Melting point	1907 °C	1083 °C
Boiling point	2672 °C	2595 °C
Hardness at 20 °C	180 - 250 [HV10]	40-45 (HB)
Modulus of Elasticity at 20 °C	294 GPa	117 GPa
Thermal Conductivity at 20 °C	93.7 W/(m·K)	391 W/m-K

3.3. Work Material

AISI 1045 die steel is a medium tensile steel supplied in the black hot rolled or normalized condition. It has a tensile strength between 570 - 700 MPa and Brinell hardness ranging between 170 and 210. AISI 1045 die steel is widely used for all industrial applications where more wear resistance and strength is required. The chemical composition of AISI 1045 die steel is depicted in Table 2.

Table 2. Chemical Composition of AISI 1045 Die Steel

Carbon %	Iron %	Manganese %	Phosphorous %	Sulphur %
0.42-0.50	98.51-98.98	0.60 - 0.90	≤ 0.040	≤ 0.050

3.4. Experimental Conditions

The range of paramters used in the present experimental work were selected based on the earlier research work and the EDM machine available for the purpose are given in Table 3.

Table 3. Experimental Conditions

Working Parameters	Description
Workpiece	AISI 1045 Die Steel (32×15×6) mm
Electrode	Cu-Cr composite electrode (10 mm diameter and 10 mm height)
Electrode composition	Cu 10% and Cr 90%
Compaction pressure	400-1200 MPa
Sintering temperature	300^0C
Powder particle size	2 to 4 microns
Dielectric	EDM-30 oil
Polarity(p)	Negative
Voltage	55-60 V
Peak current, I_p	4.5 – 10.5 A
Pulse-on,T_{on}	5-25 µs
Pulse -off,T_{off}	50-250 µs
Machining Time	10 min

3.5. Experimental Procedure

Work piece (AISI 1045 die steel) was selected for modifying its surface properties to make it wear resistant, increase its hardness and improve its surface finish. The material for the work piece was available in the form of flat piece of 32×6 mm and length 2m. It was cut into equal pieces of size 32×15 mm for experimental investigation. Work piece material was cut with the help of hydraulic press and then surface grinder was used to remove any deformation on the work piece and to straighten them.

Powder Metallurgy (P/M) technique was used to prepare the electrode made up of two powders i.e. copper and chromium with Cu 10% and Cr 90% composition. The important machining parameters such as peak current (I_p), pulse on-time (T_{on}), pulse off-time (T_{off}) and compaction pressure were selected for investigation. The effect of these input machining parameters on performance parameters such as Surface Deposition Rate (SDR), Surface Roughness (SR) and Micro hardness (MH) were studied. The surface deposition rate was obtained by the difference of the weight of the work piece before and after machining dividing by the machining time. The average surface roughness was measured for analyzing the modified surface using the surface roughness tester. Micro hardness values were measured with the help of micro hardness tester. Microstructure analysis of the modified surface layer was carried out with the help of XRD, EDS and SEM tests respectively.

3.6. Selection of Design Factors

Experimental design is an effective tool for maximizing the amount of information gained from a study while minimizing the amount of data to be collected. The experimental plans were designed on the basis of Central Composite Design (CCD) technique of RSM [5]. The factorial portion of CCD is a full factorial design with all combinations of factors at five levels (low, -1, 0, high, +1). Central points were the mid points between high and low levels. The star points were at the face of the cube portion on design that corresponds to α value of 1 and this type of design is called “rotatable CCD”. For four input variables, there are 8 star points and 7 center points and the value of alpha is 2. The compaction pressure for powder metallurgy electrode, peak current, pulse on-time and pulse off-time were selected as design factors. Each input parameter had 5 levels. The levels were selected according to the availability of the range on the EDM machine and are given below in Table 4.

Table 4. Different Levels of Parameters

Parameters	Code	Level 1	Level 2	Level 3	Level 4	Level 5
Peak current, I_p (A)	A	4.5	6	7.5	9	10.5
Pulse on-time, T_{on} (µs)	B	5	10	15	20	25
Pulse off-time, T_{off} (µs)	C	50	100	150	200	250
Compaction pressure, C_p (MPa)	D	400	600	800	1000	1200

4. Results and Discussion

The experiments were carried out on the EDM machine (G-20 Integrated type) and the results were obtained by varying the four selected input parameters and their effect was found on the performance parameters. The peak current, pulse on-time and pulse off-time were the EDM machine parameters, but the compaction pressure was the parameter of the compression testing machine used for the compaction of the electrode. The response parameters were calculated based on the data collection and the values are tabulated and given in appendix.

4.1. Surface Deposition

During the surface deposition process by the EDM process; the compacted electrode which was sintered at a particular temperature had strength less than the solid metal due to weak chemical bonding. During machining, when sufficient amount of electric current was passed

through the electrode, the powder starts disintegrating due to weak bonding and accumulates over the surface of work piece. The deposited layer thickness depends on machine settings of I_p, T_{on}, T_{off} and C_p. Suitable adjustments in machining parameters with P/M electrodes were made to achieve proper material deposition. Figure 2 shows a sample of EDMed surface under different machining conditions.

Figure 2. Edmed surface with I_p= 7.5 A,T_{on}= 15 µs, T_{off} = 150 µs, C_p= 800 MPa

Figure 2 shows the coating over the circular area of diameter 10 mm for a work piece with 2mm thick and having a thin uniform coating completely covering the area.

4.2. Analysis of Surface Deposition Rate

The electronic weighing machine was used to determine the weight of the work piece before and after machining and then divided by the machining time to obtain the surface deposition rate for each workpiece. The weighing machine used was manufactured by Essae teroka having a least count of 0.1 mg. Analysis of Variance (ANOVA) was performed on experimental data for investigating the significance and contribution of machining parameters for observed values. In this investigation, ANOVA was applied on the experiemental data obtained for studying the Surface Deposition Rate. The results obtained are depicted below in Table 5.

Table 5. Analysis of Variance of Surface Deposition Rate

Source	Sum of Squares	D_f	Mean Square	F Value	p-value Prob> F	
Model	2572.7959	14	183.7711325	116.58659	< 0.0001	Significant
A-Ip	674.6901	1	674.6901042	428.03142	< 0.0001	
B-Ton	14.931038	1	14.9310375	9.4724277	0.0077	
C-Toff	1704.7147	1	1704.714704	1081.4913	< 0.0001	
D-Cp	61.081773	1	61.08177326	38.751003	< 0.0001	
AB	2.3485563	1	2.34855625	1.489952	0.2411	
AC	18.511506	1	18.51150625	11.74392	0.0037	
AD	0.3813062	1	0.38130625	0.2419052	0.6300	
BC	0.4935062	1	0.49350625	0.3130862	0.5841	
BD	0.7788062	1	0.77880625	0.4940839	0.4929	
CD	0.6683063	1	0.66830625	0.4239814	0.5248	
A^2	56.588911	1	56.58891096	35.900678	< 0.0001	
B^2	18.369983	1	18.36998343	11.654136	0.0038	
C^2	0.517284	1	0.517284011	0.3281711	0.5752	
D^2	53.197225	1	53.19722514	33.748952	< 0.0001	
Residual	23.643945	15	1.576263016			
Lack of Fit	23.534145	10	2.353414524	107.16824	< 0.0001	Not significant
Pure Error	0.1098	5	0.02196			
Cor Total	2596.4398	29				

The regression equations were developed for the surface deposition rate using mathematical models from the design software.

The mathematical equation in terms of input process parameters obtained is:

$$\begin{aligned} SDR = {} & -56.438857 + 15.531289 \times I_p \\ & + 1.7960819 \times T_{on} - 0.0504751 \times T_{off} \\ & + 0.0594812 \times C_p - 0.0510833 \times I_p \times T_{on} \\ & - 0.0143417 \times I_p \times T_{off} + 0.0005146 \times I_p \times C_p \\ & - 0.0007025 \times T_{on} \times T_{off} \\ & - 0.0002206 \times T_{on} \times C_p + 2.044e^{-05} \times T_{off} \times C_p . \end{aligned} \quad (1)$$

The graphical representation of the above SDR model is shown in Figure 3.

From the Figure 3, it is clear that the predicted values are almost equal to the actual SDR values except for the experimental values of experiment no. 3, 6, 15 and 27 respectively. The effect of individual parameter on SDR was found by plotting the perturbation graph for the combined effect of input parameters on SDR as shown in Figure 4 and are briefly discussed below.

(a) Effect of peak current

The curve with denotion (A) shows the effect of peak current on SDR. It was observed that SDR increases with increase in peak current values because with the increase in discharge energy across the spark gap, more heat is

transferred and it causes more and more disintegration of powder from the sintered electrode which gets mixed with the work piece surface and gets collected.

(b) Effect of pulse on-time

The curve with denotion (B) shows the effect of pulse on-time on SDR. SDR increases slightly with the increase in pulse on-time due to increase in heat generation across the spark gap. The rate of evaporation and vapourisation of electrode increases for both P/M electrode and work piece. Pulse on-time is the time during which the machining is carried out. Hence, increase in pulse on-time means the increase in the heating temperature for longer time for same machining time.

(c) Effect of pulse-off time

The curve with denotion (C) shows the effect of pulse off-time on SDR. SDR decreases with increase in pulse off-time because with increase in pulse off-time there is more efficient flushing, but during this time there is no machining. It reduces the heat energy generated across the spark and decreases the melting and evaporation of both electrode and work piece.

(d) Effect of compaction pressure

The effect of compaction pressure on SDR is shown by the curve with denotion (D). SDR slightly decreases with increase in compaction pressure because sintered electrode with high compaction pressure gives less SDR and high SDR with low compaction pressure. This low SDR is because with more compaction pressure, the copper and chromium particles bind together strongly and gain high green compact strength which requires more energy to disintegrate while machining and gets deposited on the work piece surface.

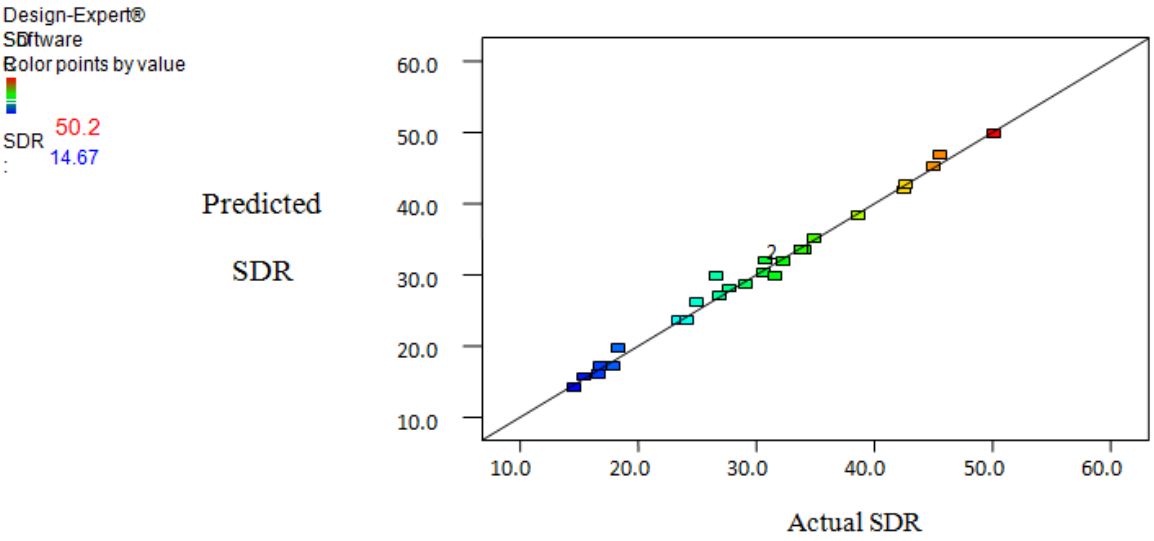

Figure 3. Predicted Vs. Actual Surface Deposition Rate

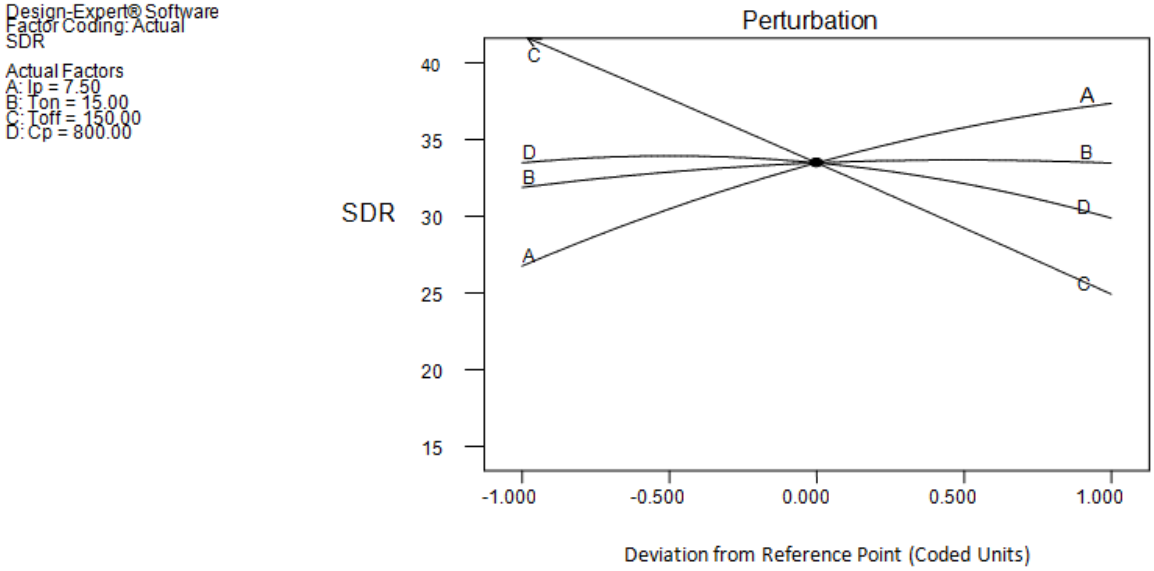

Figure 4. Perturbation Graph of Surface Deposition Rate

4.3. Analysis of Surface Roughness

Surface roughness tester was used in the experiment for determining the roughness value of the machined samples in microns. The measuring length of the tester was 10 mm and the cut off length was 2.5 mm. Analysis of variance (ANOVA) was also performed on experimental data for investigating the significance and contribution of the machining parameters on the surfaces roughness values. The Analysis of Variance of surface roughness so obtained is given in Table 6.

Table 6. Analysis of Variance of Surface Roughness

Source	Sum of Squares	D_f	Mean Square	F Value	p-value Prob > F	
Model	11.10305	14	0.793074995	346.76579	< 0.0001	Significant
A-Ip	2.577426	1	2.577426042	1126.9592	< 0.0001	
B-Ton	0.9420844	1	0.942084375	411.91896	< 0.0001	
C-Toff	5.19033	1	5.190330042	2269.4309	< 0.0001	
D-Cp	0.4388784	1	0.438878449	191.89614	< 0.0001	
AB	0.1374556	1	0.137455563	60.10136	< 0.0001	
AC	0.6072306	1	0.607230563	265.50677	< 0.0001	
AD	0.3742381	1	0.374238063	163.63264	< 0.0001	
BC	0.0002031	1	0.000203062	0.0887875	0.7698	
BD	0.0774231	1	0.077423062	33.852623	< 0.0001	
CD	0.5044551	1	0.504455063	220.569	< 0.0001	
A^2	0.1320099	1	0.1320099	57.720287	< 0.0001	
B^2	0.007029	1	0.007028983	3.0733673	0.1000	
C^2	0.0049884	1	0.004988409	2.1811424	0.1604	
D^2	0.0083207	1	0.008320677	3.6381506	0.0758	
Residual	0.0343059	15	0.002287062			
Lack of Fit	0.0259991	10	0.00259991	1.5649226	0.3243	Not significant
Pure Error	0.0083068	5	0.001661367			
Cor Total	11.137356	29				

The regression equation were developed for the surface roughness values using mathematical models.

The final mathematical equation of SR in terms of input process parameters is:

$$\begin{aligned} SR = {} & 18.440041 - 1.2889479 \times I_p + 0.0978394 \times T_{on} \\ & - 0.0411694 \times T_{off} - 0.009197 \times C_p \\ & - 0.0123583 \times I_p \times T_{on} + 0.0025975 \times I_p \times T_{off} \\ & + 0.0005098 \times I_p \times C_p - 1.425e^{-5} \times T_{on} \times T_{off} \\ & + 6.956e^{-5} \times T_{on} \times C_p + 1.776e^{-5} \times T_{off} \times C_p \\ & + 0.0305595 \times {I_p}^2 - 0.0006346 \times {T_{on}}^2 \\ & - 5.346e^{-6} \times {T_{off}}^2. \end{aligned} \quad (2)$$

The graphical representation of the above said surface roughness model is depicted below in Figure 5.

From Figure 5, it is observed that the surface roughness values for experiment no. 3 lie above and 13 below the origin line respectively and the rest of the values are on the line. The effect of individual parameter on SR was found by plotting the perturbation graph as shown in Figure 6.

The effect of input machining parameters observed on surface roughness are discussed below:

(a) Effect of peak current

The curve with denotion (A) shows the effect of peak current on SR. It is revealed from the figure that with increase in peak current, the surface roughness slightly decreases because at lower peak current the surface deposition is very less which means that surface roughness of the machined surface is high. At higher value of peak current, the surface roughness of the work piece surface is less due to the more surface deposition by the powder disintegration from the powder sintered electrode. The heat energy generated increases across the spark gap with more heat energy, powder disintegration is fast and SR decreases. Peak current increases the discharge energy which decreases the surface roughness.

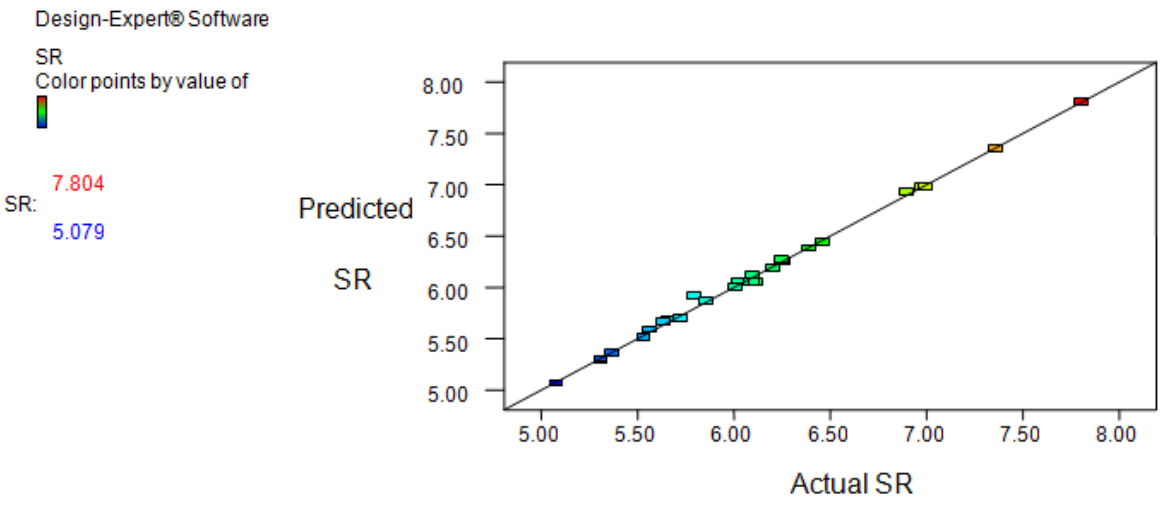

Figure 5. Predicted Vs. Actual Surface Roughness Values

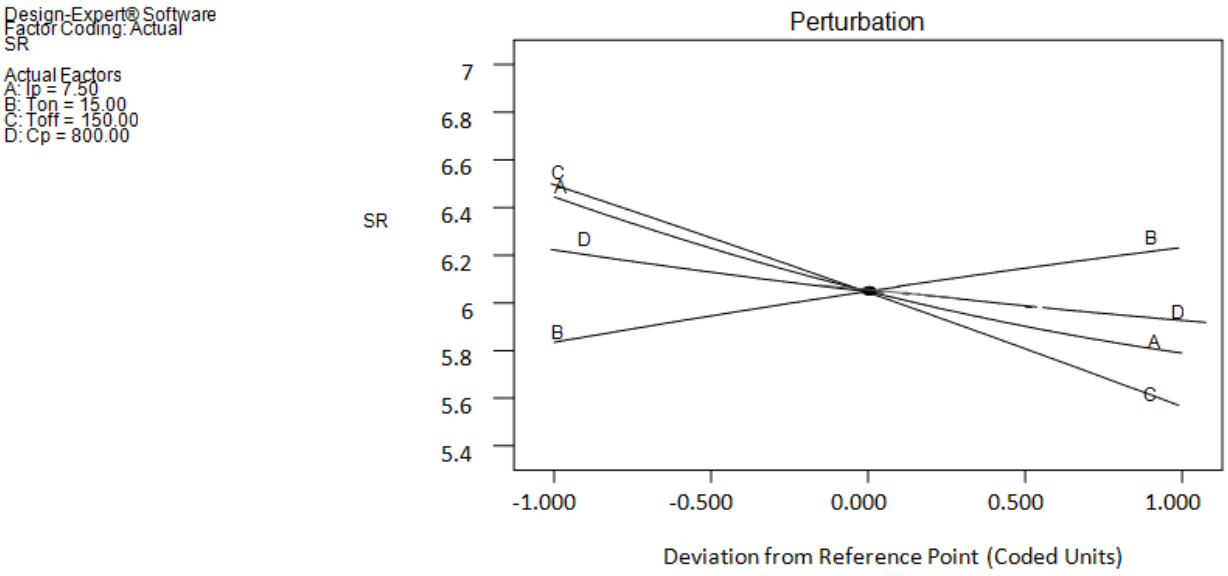

Figure 6. Perturbation Graph of Surface Roughness

(b) Effect of pulse-on time

The curve with denotion (B) shows the effect of pulse on-time on SR. The machining time is less which reduces the surface deposition of machined surface. At higher values of pulse on-time, the surface roughness increases due to more surface deposition.

(c) Effect of pulse-off time

The curve with denotion (C) shows the effect of pulse off-time on SR. With increase in pulse off-time, the machining time decreases which reduces the surface deposition and the surface roughness.

(d) Effect of compaction pressure

The curve with denotion (D) shows the effect of compaction pressure on SR. With high compaction pressure the powders are bonded strongly which does not disintegrate easily and the surface deposition is less and decreases the surface roughness. At low compaction pressures, the powder disintegrates easily and increases the surface roughness. A high tool energy density results in high tool consumption, large stock material drops on work piece which decreases the surface roughness.

4.4. Analysis of Micro Hardness

Micro hardness tester manufactured by Mitutoyo, Japan having measuring indentations of ×10, ×50 and × 100 was for for measuring the micro hardness. Micro hardness of the base metal was 32 HRc. The micro hardness of the modified surface of the coating was found for knowing the wear characteristics of the coating. The ANOVA values for micro hardness are given in Table 7.

Table 7. Analysis of Variance of Micro Hardness

Source	Sum of Squares	D_f	Mean Square	F Value	p-value Prob> F	
Model	969.67112	10	96.96711182	44.186375	< 0.0001	Significant
A-Ip	260.04167	1	260.0416667	118.49686	< 0.0001	
B-Ton	100.04167	1	100.0416667	45.5874	< 0.0001	
C-Toff	425.04167	1	425.0416667	193.68474	< 0.0001	
D-Cp	34.171118	1	34.17111818	15.571236	0.0009	
AB	27.5625	1	27.5625	12.559794	0.0022	
AC	45.5625	1	45.5625	20.762108	0.0002	
AD	33.0625	1	33.0625	15.066057	0.0010	
BC	0.0625	1	0.0625	0.0284803	0.8678	
BD	5.0625	1	5.0625	2.3069009	0.1453	
CD	39.0625	1	39.0625	17.800162	0.0005	
Residual	41.695548	19	2.194502552			
Lack of Fit	36.362215	14	2.597301083	2.4349698	0.1665	Not significant
Pure Error	5.3333333	5	1.066666667			
Cor Total	1011.3667	29				

The regression equations were developed for the surface deposition rate using mathematical models from the design software.

The mathematical equation for micro hardness values in terms of input process parameters are as follows:

$$MH = 149.69313 - 6.7777778 \times I_p + 1.2333333 \times T_{on} - 0.3816667 \times T_{off} - 0.0741956 \times C_p - 0.175 \times I_p \times T_{on} + 0.0225 \times I_p \times T_{off} + 0.0047917 \times I_p \times C_p + 0.00025 \times T_{on} \times T_{off} + 0.0005625 \times T_{on} \times C_p + 0.0001563 \times T_{off} \times C_p. \quad (3)$$

The graphical representation of the above said micro hardness model is given below in Figure 7.

From Figure 7, it was found that micro hardness values for experiment no. 3, 8, 17, 27 lie above and 21 below the origin line respectively and the rest of the values are on the line. The variation of individual parameter on MH was found by plotting the perturbation graph as shown in Figure 8.

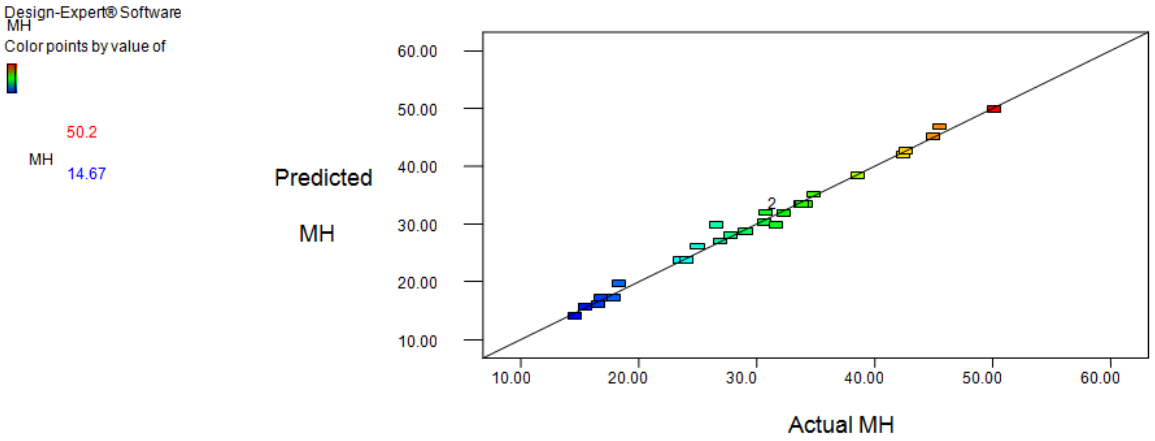

Figure 7. Predicted Vs. Actual Values of Micro Hardness

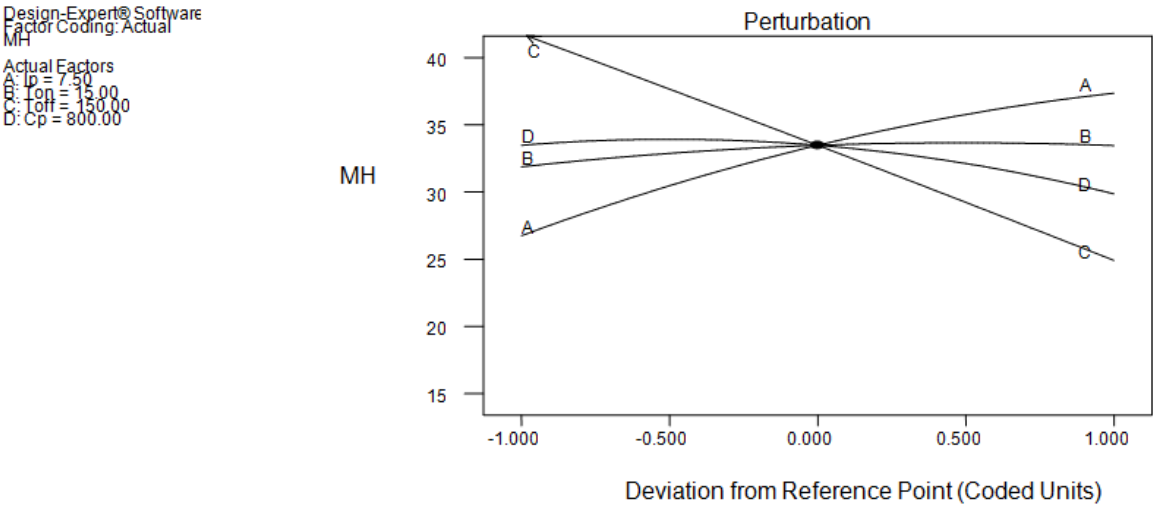

Figure 8. Perturbation Graph of Micro Hardness

The effect of input parameters on performance characteristics are briefly discussed below:

(a) Effect of peak current

The effect of peak current on MH is depicted by the curve with denotion (A). With high peak current values, the surface deposition is more and the chromium combines with the carbon obtained from the deionization of dielectric fluid to form chromium carbide. With heavy deposition, the surface layer becomes soft which reduces the micro hardness values of the deposited layer.

(b) Effect of pulse on-time

The curve with denotion (B) shows the effect of pulse on-time on MH. When the pulse on-time is increased, the surface deposition increases and the micro hardness decreases due to increased machining time and thick layer.

(c) Effect of pulse off-time

The curve with denotion (C) shows the effect of pulse off-time on MH. The increase in pulse off-time decreases the machining time which decreases the micro hardness of the work piece.

(d) Effect of compaction pressure

The variation of compaction pressure is shown by the curve with denotion (D). With negative polarity of electrode and at low compaction pressure, copper and chromium particles adhere to the work piece which increases its micro hardness. But with high compaction pressure, particles adherence to work piece is less which reduces the micro hardness. Discharge spot results in wider melting zone. Consequently, particles adhere to the work piece surface. With high compaction pressure, electrode particles are bonded together strongly but at low compaction pressure, SDR is more which increases the micro hardness of the work piece. There is decrease in micro hardness value along the depth of work piece and remains same along the horizontal direction.

4.5. Characteristics of Machined Surface

Resolidification occur at high temperatures during EDM process which changes the micro-structure of the

machined surface layer known as Heat Affected Zone (HAZ). There are three main types of hardness layers : recast layer, intermediate and unaffected matrix layer in decreasing hardness order.

(i) XRD Analysis

X-ray diffraction is a rapid analytical technique primarily used for phase identification of a crystalline material and provide information on unit cell dimensions. The XRD graph of EDMed work piece is shown in Figure 9.

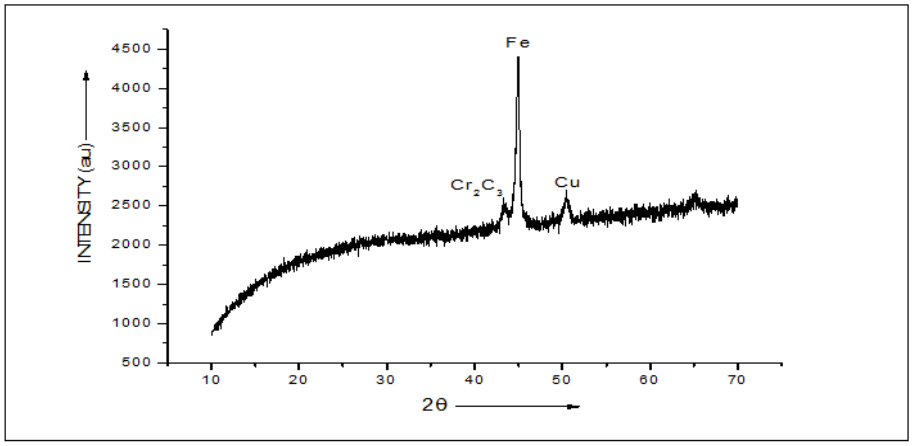

Figure 9. X-RAY Diffraction of EDMed Surface

Figure 9 shows the Bragg's angle on X-axis and the intensity (au) on Y-axis. The XRD analysis shows that when the intensity is increased chromium carbide is formed during machining and the same compound is responsible for the increase in hardness of the EDMed surface. The diffraction peak of Fe (2θ) is 45^0, the diffraction peak of chromium carbide (Cr_2C_3) is 42^0 and copper(Cu) is 50^0 formed in the modified surface respectively.

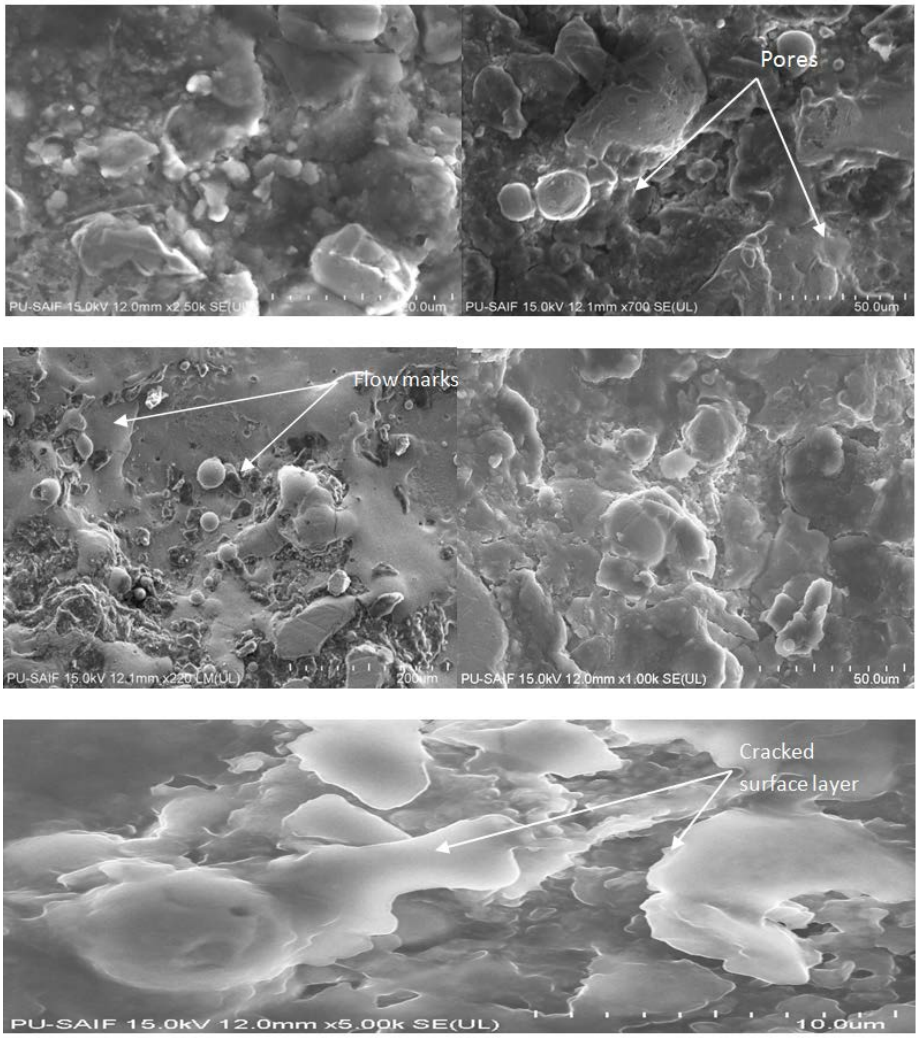

Figure 10. SEM Microscopic view of the EDMed Surface

(ii) SEM Analysis

The Scanning Electron Microscope (SEM) uses a focused beam of high-energy electrons to generate a variety of signals at the surface of solid specimens. The SEM microscopic views were developed to compare the modified surface with the base. The SEM shows the crack free surface layer, pores and flow marks formed during machining are depicted in Figure 10.

4.6. Parametric Optimization

The optimum solution was obtained by DOE software 8 by considering the relation between the four input parameters and response variables. The optimum parameter settings so obtained are given below in Table 8. The optimum value of SDR i.e. 45.1529 mg/min was obtained in experiment no. 1 and 27, minimum surface roughness of 6.19 microns was obtained in experiment no. 2, 6 and16, maximum micro hardness of 61 HRc was found in experiment no.1, 2, 16, 21 and 29 respectively.

Table 8. Optimum Values of Parameters in Design Space

Parameter	Optimum value
Peak current	9 A
Pulse on time	10 µs
Pulse off time	100 µs
Compaction pressure	600 MPa
SDR	45.15 mg/min
SR	6.19 microns
MH	61 HRc

Further random experiments were carried out for comparison between experimental and predicted values and the percentage error was noted between the predicted and actual values are as given in Table 9. The maximum percentage error noted was 0.13 for SDR, 0.16 for SR and 0.09 for MH which shows a very good agreement between the experimental and predicted values.

Table 9. Comparison of Actual and Predicted Values of Response Parameters

Parameter	Ip	Ton	Toff	Cp	SDR	SR	MH
Predicted	9	10	100	600	45.15	6.19	61.71
Actual	9	10	100	600	45.21	6.18	61.65
% error					0.13	0.16	0.09

5. Conclusions

A total 30 experiments were conducted using powder metallurgy electrodes on AISI 1045 die steel. The conclusions based on the experimental results are as follows:

(i) Maximum surface deposition rate (SDR) obtained was 45.15 mg/ min.

(ii) Minimum surface roughness (SR) obtained was 6.19 microns.

(iii) Maximum micro hardness (MH) obtained was 61 HRc.

(iv) The optimal combination of input parameters is peak current 9A, pulse on-time 10 micro seconds, pulse off-time 100 micro sseconds and compaction pressure of 600 MPa.

(v) The powder metallurgy electrode provided two times increase in hardness of the work piece surface. The base material hardness was 32HRc and the hardness of the modified surface was 61HRc.

(vi) It was found that pulse off-time had greater effect on surface deposition and micro hardness followed by peak current, pulse on-time and compaction pressure respectively.

(vii) It was also found that pulse off-time had greater effect on surface roughness followed by peak current, pulse on-time and compaction pressure respectively.

(viii) By the use of copper-chromium composite electrode, chromium particles gets collected on the surface which modified the work piece surface by increasing its corrosion and wear resistance.

(ix) The favourable conditions for surface deposition by EDM were peak current less than 10 A, pulse on-time below 50 micro seconds and pulse off-time above 50 micro seconds.

References

[1] Patowari P.K., Saha P. and Mishra P.K., "An experimental investigation of surface modification of C-40 steel using W–Cu powder metallurgy sintered compact tools in EDM", *The International Journal of Advanced Manufacturing Technology*, 2015, pp. 1-18.

[2] Hayakawa, Shinya, Ricardo, Ori I., Itoigawa F., Nakamura T. and Matsubara T.,"Micro fabrication using EDM deposition", *Initiatives of Precision Engineering at the Beginning of a Millennium*, 2002, pp. 72-76.

[3] Patowari P.K., Saha P. and Mishra P.K., "Taguchi analysis of surface modification technique using W-Cu powder metallurgy sintered tools in EDM and characterization of the deposited layer", *International Journal Of Advanced Manufacturing Technology*, Vol. 54, 2011, pp. 593-604.

[4] Singh A. and Kumar S., "Surface alloying of H11 die steel by tungsten using EDM process", *International Journal Of Advanced Manufacturing Technology* ,Vol. 78, 2015, pp. 1585-1593.

[5] Sidhu H. S., Banwait S. S. and Laroiya S. C., "Development of RSM Model in Surface Modification of En-31 Die Steel Material Using Copper-Tungsten Powder Metallurgy Semi-Sintered Electrodes by EDM Process", *American Journal of Mechanical Engineering*, Vol. 1(6), 2013, pp. 155-160.

[6] Gill A.S. and Kumar S., "Surface alloying of H11 die steel by tungsten using EDM process", *International Journal of Advanced Manufacturing Technology*, Vol.78, 2015, pp.1585-1593.

[7] Abrol, Abhishek and Sharma S., "Effect of Chromium powder mixed dielectric on performance characteristic of AISI D2 die steel using EDM", Vol. 4, 2015, pp.232-246.

[8] Pradhan M.K., "Estimating the effect of process parameters on MRR, TWR and radial overcut of EDMed AISI D2 tool steel by RSM and GRA coupled with PCA", *International Journal of Advanced Manufacturing Technology*, Vol. 68, 2013, pp. 591-605.

[9] El-Taweel T.A., "Multi-response optimization of EDM with Al–Cu–Si–TiC P/M composite electrode", *International Journal Of Advanced Manufacturing Technology*, Vol. 24, 2009, pp. 100-113.

[10] Patowari P.K., Saha P. and Mishra P.K., "Artificial neural network model in surface modification by EDM using tungsten–copper powder metallurgy sintered electrodes", *International Journal Of Advanced Manufacturing Technology* ,Vol. 51, 2010, pp. 627-638.

[11] Caydas U. and Hascalik A., "Modeling and analysis of electrode wear and white layer thickness in die-sinking EDM process through response surface methodology", *International Journal of Advanced Manufacturing Technology*,Vol. 38, 2008, pp. 1148-1156.

Appendix : Experimental Design Matrix And Collected Data

Run	I_p (A)	T_{on} (µs)	T_{off} (µs)	C_p (MPa)	SDR (mg/min)	SR (microns)	MH (HRc)
1	9	10	100	600	45.03	6.202	62
2	7.5	15	150	800	33.9	6.107	62
3	7.5	15	150	1000	26.57	5.793	57
4	7.5	25	150	800	32.33	6.393	64
5	7.5	15	150	800	33.8	6.059	60
6	6	20	200	600	18.33	6.1	62
7	7.5	15	150	800	34.17	6.033	60
8	6	10	100	600	30.83	7.361	73
9	6	10	200	600	16.8	5.658	56
10	9	20	200	600	26.93	5.367	54
11	6	10	200	1000	14.67	5.313	54
12	7.5	15	50	800	50.2	6.897	68
13	9	10	200	1000	23.5	5.533	56
14	7.5	5	150	800	29.1	5.563	55
15	9	10	200	600	25.03	5.31	54
16	7.5	15	150	800	33.8	6.12	62
17	9	10	100	1000	42.5	5.722	59
18	6	20	100	1000	30.7	6.972	70
19	6	10	100	1000	27.8	6.263	63
20	7.5	15	150	400	31.67	6.462	64
21	9	20	100	1000	42.67	6.097	62
22	7.5	15	150	800	33.78	6.044	60
23	6	20	100	600	34.9	7.804	**78**
24	7.5	15	150	800	33.83	6.02	60
25	9	20	200	1000	24.1	5.858	58
26	4.5	15	150	800	17.9	6.998	70
27	9	20	100	600	**45.53**	6.251	62
28	10.5	15	150	800	38.63	5.635	56
29	6	20	200	1000	15.47	6.008	62
30	7.5	15	250	800	16.63	**5.079**	54